

Computational analysis of molecular properties and spectral characteristics of cyano-containing liquid crystals: Role of alkyl chains

P. Lakshmi Praveen and Durga P. Ojha*

Post-Graduate Department of Physics, Liquid Crystal Research Laboratory, Andhra Loyola College, Vijayawada-520 008, A.P., India

(Received 7 February 2011; published 27 May 2011)

The electronic transitions in the uv-visible range of 4'-*n*-alkyl-4-cyanobiphenyl (*n*CB) with propyl, pentyl, and heptyl groups, which are of commercial and application interests, have been studied. The uv-visible and circular dichroism spectra of *n*CB ($n = 3,5,7$) molecules have been simulated using the time dependent density functional theory Becke3-Lee-Yang-Parr hybrid functional-6-31 + G (d) method. Mulliken atomic charges for each molecule have been compared with Loewdin atomic charges to analyze the molecular charge distribution and phase stability. The highest occupied molecular orbital and lowest unoccupied molecular orbital energies corresponding to the electronic transitions in the uv-visible range have been reported. Excited states have been calculated via the configuration interaction single level with a semiempirical Hamiltonian (intermediate neglect of differential overlap method, as parametrized by Zerner and co-workers). Further, two types of calculations have been performed for model systems containing single and double molecules of *n*CB. Furthermore, the dimer complexes during the different modes of molecular interactions have also been studied. The interaction energies of dimer complexes have been taken into consideration in order to investigate the most energetically stable configuration. These studies are helpful for understanding the role and flexibility of end chains, in particular, phase behavior and stability.

DOI: [10.1103/PhysRevE.83.051710](https://doi.org/10.1103/PhysRevE.83.051710)

PACS number(s): 61.30.Cz, 64.70.M-

I. INTRODUCTION

Liquid crystals (LCs), as the crystals that flow, have gained much prominence in multidirectional facets with realistic models [1,2] and excited practical applications. These strong anisotropic molecular materials enthrall theoretical physicists [3], crystallographers, [4], and device engineers. The foremost focus is to explore novel LC materials with differing molecular chemistry in order to study their practicability in technological appliances. The multiphase and multidisciplinary aspects of LCs are guides to link basic physics with other scientific disciplines and technologies. Applications for this sort of material are still being discovered and are persistent in providing effective keys to scores of different setbacks. However, these organic designs are fairly appealing from an elemental research point of view as complex fluids with intriguing symmetries and unusual elastic properties, which constitute highly motivating theoretical challenges [5]. A theoretical insight into the electronic structure properties, which have a prominent influence on the desired material parameters, is required for further experimental investigations.

LCs are used extensively for direct-view displays, projection displays, and photonic devices. Material and phase stabilities are a primary concern for all devices desiring to have a long operational lifetime. In direct-view displays, uv light is often used. The uv light causes a gradual degradation of the LC molecules so that the consequent electro-optic effects are altered. Therefore, it is critical to identify the ultimate LC material failure mechanism and to search for molecular structures that can withstand a longer uv exposure. The most common nematic LC structure for displays consists of an alkyl chain, one or two cyclohexane rings, a phenyl ring, and a polar group. The aromatic ring system not only

imparts structural anisotropy, but also plays a central role in determining the electrical, magnetic, and optical properties of the bulk materials. For the active matrix liquid-crystal display (LCD) applications, fluoro is the preferred polar group as it exhibits a high resistivity, a low viscosity, and a low birefringence [6,7]. However, both cyano (CN) [8] and isothiocyanate [9] are the popular preferences for use in most passive matrix LCDs, as they exhibit a large dipole moment to the normally weakly polar or nonpolar core, give excellent chemical stability, and contribute to the display and photonic applications.

The simulation of uv-visible spectra by computational chemistry tools is particularly appealing since contemporary approaches are proficient to provide results with accuracy comparable to that obtained by experiments. Of particular importance, in this sense, methods based on time dependent density functional theory (TD-DFT) provide very accurate results [10,11]. Such approaches allow for the calculation of electronic transitions between the ground state and the different excited states, which gives the energies of the corresponding radiations. Each transition can be enlarged with a Gaussian shape due to several factors, such as thermal excitement, natural line width, etc.

The present paper deals with the theoretical evaluation of the key electronic quantities and optical properties of nematogenic 4'-*n*-alkyl-4-cyanobiphenyl (*n*CB) molecules with propyl (3CB), pentyl (5CB), and heptyl (7CB) groups, which are of commercial and application interests. In particular, it concentrates on the variations in the uv-visible absorption spectra and circular dichroism (CD) spectra with respect to homolog number. All the molecules show strong absorptions in the uv range that are very sensitive to the changes in the alkyl chain length. The highest occupied molecular orbital (HOMO) and lowest unoccupied molecular orbital (LUMO) energies have also been reported for all single

*E-mail address: durga_ojha@hotmail.com

molecules and dimer complexes during the different modes of molecular interactions. An attempt has been made to find the most energetically favorable configuration in each mode of interaction. Furthermore, the role of alkyl chains has been analyzed in altering the electronic and optical properties of the systems. An examination of thermodynamic data has revealed that the 3CB molecule exhibits a nematic-isotropic transition temperature at 303.3 K [12], 5CB exhibits a nematic-isotropic transition temperature at 308.2 K [13], and 7CB exhibits a nematic-isotropic transition temperature at 315.8 K [13].

II. COMPUTATIONAL METHODOLOGY

The studied model composed the monomer and dimer assemblies of n CB ($n = 3,5,7$). Geometry optimizations have been performed using the density functional theory (DFT) approach [10], in particular, the Becke3-Lee-Yang-Parr hybrid functional (B3LYP) exchange-correlation functional and the 6-31G (d) basis set. The DFT approach was originally developed by Hohenberg and Kohn [14], Kohn and Sham [15], and Jones and Gunnarson [16] to provide an efficient method of handling the many-electron system. The theory allows us to reduce the problem of an interacting many-electron system to an effective single-electron problem. On the basis of the DFT geometries, the electronic structures and the excited states have been calculated at a semiempirical Hartree-Fock level with the intermediate neglect of the differential overlap method, as parametrized by Zerner [17,18] coupled with the configuration interaction (CI) single level of approximation including all $\pi \rightarrow \pi^*$ single excitations. This has been found adequate for determining the uv-visible absorption and CD spectra.

Common structural parameters of the systems, such as bond lengths and bond angles have been taken from published crystallographic data [12], [19]. Charge distributions of the molecules have been calculated by performing Mulliken and Loewdin population analyses. The mesomorphic behavior and the nematic phase stability have been predicted through the calculated local charge distributions. Based on the optimal geometry obtained for each molecule, a systematic examination of interactions between a pair of isolated molecules has been carried out. The absorption maxima and HOMO and LUMO orbitals have been analyzed to describe the electronic properties of the systems.

III. RESULTS AND DISCUSSION

The geometric structures of n CB ($n = 3,5,7$) have been shown in Fig. 1. The structures have been constructed based on the published crystallographic data with the standard values of bond lengths and bond angles [12,19]. Mulliken and Loewdin atomic net charges have been calculated, and the group charges from both methods have been reported in Table I. The molecular charge distribution and phase stability of the molecules have been analyzed as given below.

A. Molecular charge distribution and phase stability

It is expected that the specific charge distributions and electrostatic interactions in mesomorphic molecules play an influential role in the configuration of various mesophases. An appropriate modeling of this fundamental molecular feature

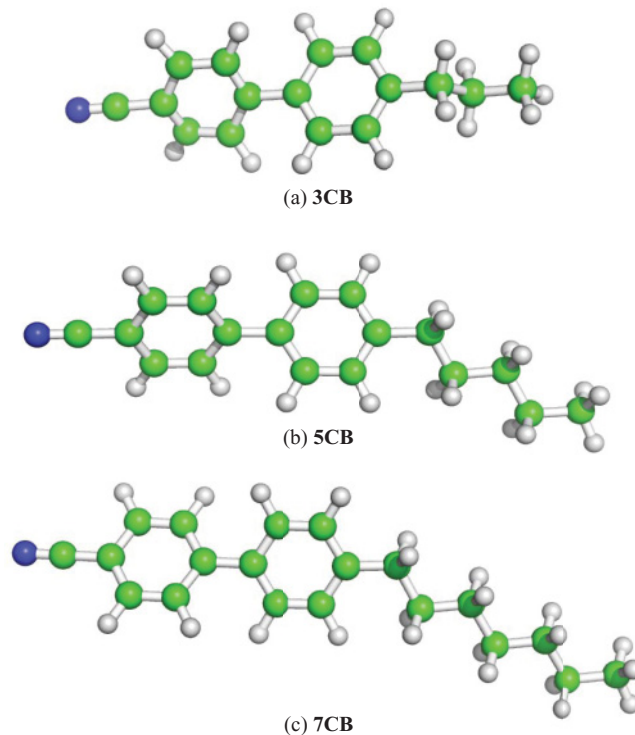


FIG. 1. (Color online) The geometric structures of (a) 3CB, (b) 5CB, and (c) 7CB molecules.

relies on the possibility of assigning a partial charge to all atomic centers [20]. To parametrize the molecular interactions for computational studies, atom positioned partial charges are helpful [21]. The possibility for taking a detailed look at the electronic structure of the molecules can be performed by determining atom-based partial charges, which are not quantum mechanical observables. These charges represent the electrostatic molecular interactions very well, but they do not show the real charge distribution in the molecule.

Since group charges are needed to explain the behavior of mesogens, Mulliken population analysis (MPA), which partitions the total charge among the atoms in the molecule, has been performed and has been compared with those obtained from Loewdin population analysis (LPA). However, there is much agreement among the methods when it comes to the group charges of each molecule. The results show that the alkyl chain plays a major role in the charge distribution. From Table I, it is evident that the charges on the core and CN group are almost the same (especially for $n = 5,7$). The core in 3CB is neutral (as per MPA). In this case, alkyl chains will be strongly

TABLE I. Mulliken (M) and Loewdin (L) group charges and nematic-isotropic transition temperatures for n CB ($n = 3,5,7$) molecules.

Molecule	Core		CN		Alkyl		T (K) [12,13]
	M	L	M	L	M	L	
3CB	0.000	0.151	-0.213	-0.197	0.213	0.046	303.3
5CB	-0.204	0.049	-0.185	-0.172	0.389	0.123	308.2
7CB	-0.232	0.048	-0.185	-0.172	0.417	0.124	315.8

attracted by the negatively charged CN group. Furthermore, the positively charged alkyl chains in 5CB and 7CB will be strongly attracted by the negatively charged core as well as the CN group, causing the formation of longer units in the mesophase (as per both MPA and LPA). Hence, the phase stability is expected to be high for higher homologs ($n = 5, 7$). The nematic-isotropic transition temperature (T_{N-I}) of n CB ($n = 3, 5, 7$) molecules reported in the literature (Table I) supports this finding.

B. Electronic absorption spectrum

One of the most exciting developments in LC science and technology is the possibility of using light instead of electricity to control the behavior of a material [22,23]. Increasing the number of carbon atoms in the end chain is the widely used technique in order to alter the physical properties of LC molecules. The description of molecular quantities by quantum chemical methods underlies some principal restrictions, i.e., a compromise exists between the complexity of the systems studied and the accessible theoretical accuracy. In the calculation of electronic spectra, the CI method is widely employed. Using a CI method in combination with a semiempirical model Hamiltonian, an evaluation of absorption spectra of large organic molecules and LCs becomes possible [24–26]. It is expected that the absorption spectrum of a LC molecule containing a single phenyl ring would exhibit similarities to that of an isolated benzene molecule. The principal absorption bands in the molecules are due to the $\pi \rightarrow \pi^*$ transitions in the benzene analogous part of the molecule [27]. In general, these benzenelike transitions are roughly conserved in the model systems studied, but they are influenced by the conjugation length, the degree of conjugation, and the different substituents. The analysis of electronic absorption spectra of isolated molecules is given below.

1. 3CB

The electronic absorption spectrum of 3CB is shown in Fig. 2. In the uv region, four strong absorptions at 212.30 nm

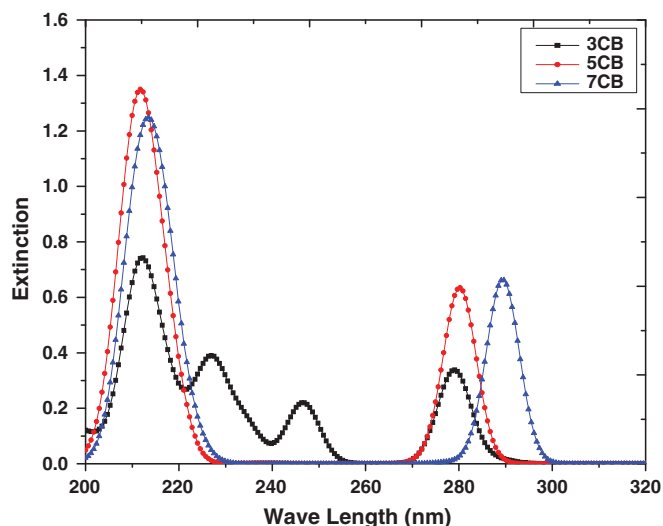


FIG. 2. (Color online) Electronic absorption spectra of n CB ($n = 3, 5, 7$) molecules. Extinction unit, $10^4 \text{ dm}^3 \text{ mol}^{-1} \text{ cm}^{-1}$.

(λ_1), 226.95 nm (λ_2), 246.88 nm (λ_3), and 279.10 nm (λ_4) have been observed. However, no absorption has been observed in the visible region. The strongest band appears in a region of 201.76–222.27 nm with absorption maxima (λ_{max}) at 212.30 nm. This band arises from the HOMO \rightarrow LUMO transition and is assigned as the $\pi \rightarrow \pi^*$ transition in the molecule. The other absorptions corresponding to λ_2 , λ_3 , and λ_4 also indicate $\pi \rightarrow \pi^*$ transitions in the molecule. The oscillator strengths (f) corresponding to four strong absorptions are 0.19, 0.36, 0.22, and 0.33, respectively. Therefore, these transitions contribute higher oscillator strength corresponding to the second absorption band (λ_2).

2. 5CB

Figure 2 shows the electronic absorption spectrum of the 5CB molecule. The two prominent bands have been identified in the uv region with absorption maxima at 211.72 nm (λ_1) and 280.27 nm (λ_2). The strongest band has been observed from 200 to 224.02 nm with absorption maxima at 211.72 nm (λ_1). This band arises due to the HOMO \rightarrow LUMO transition and is assigned as a $\pi \rightarrow \pi^*$ transition in the molecule. The other band also indicates the possibility for a $\pi \rightarrow \pi^*$ transition. Furthermore, the oscillator strength corresponding to λ_1 and λ_2 are 0.64 and 0.63, respectively. Hence, the 5CB molecule contributes a higher f value corresponding to $\pi \rightarrow \pi^*$ transition at λ_1 . This is in good agreement with the experimental data reported in the literature [28] for the 5CB molecule that exhibits two $\pi \rightarrow \pi^*$ transitions at 210 and 280 nm, respectively.

3. 7CB

A graphical representation of the absorption spectrum of the 7CB molecule is shown in Fig. 2. Evidently, two strong absorption bands have been noticed in the uv region with absorption maxima at 213.48 nm (λ_1) and 289.65 nm (λ_2). The strongest band has been observed in a region from 200 to 230.47 nm with absorption maxima at 213.48 nm, which arises due to the transition between HOMO \rightarrow LUMO energy states. This can be assigned as a $\pi \rightarrow \pi^*$ transition in the molecule. However, the other band also indicates the possibility of a $\pi \rightarrow \pi^*$ transition. The oscillator strength (f) corresponding to two strong absorptions λ_1 and λ_2 are 0.68 and 0.66, respectively. Furthermore, it shows a higher f value corresponding to the strongest absorption λ_1 . The estimated wavelengths are in good agreement with the experimental values reported in the literature [29].

C. Circular dichroism spectrum

The CD spectra of n CB ($n = 3, 5, 7$) molecules have been shown in Fig. 3. The 3CB molecule exhibits three strong absorption bands (Fig. 3) in the uv region at 215.23 nm (λ_1), 233.98 nm (λ_2), and 279.10 nm (λ_3) with absorption maxima (λ_{max}) at 233.98 nm. The strongest absorption band has been noticed in a region from 224.61 to 251.56 nm with absorption maximum at λ_2 . The rotatory strengths (R) corresponding to three absorptions are 29.25, 44.43, and 16.78, respectively. Furthermore, two strong absorption bands have been noticed for 5CB at 213.48 nm (λ_1) and 280.27 nm (λ_2) with absorption

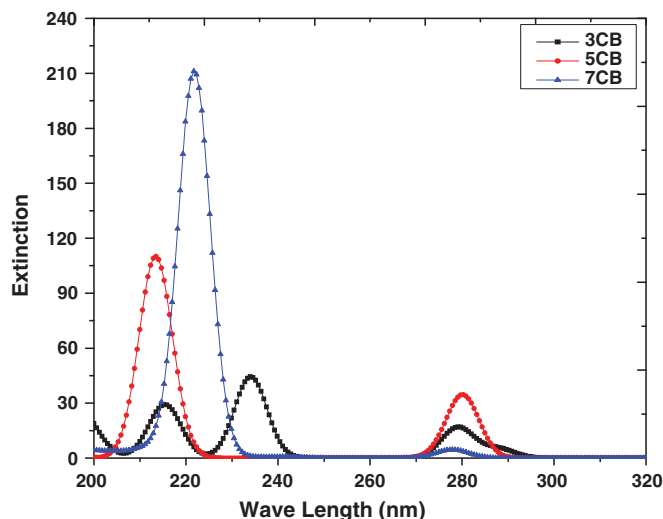


FIG. 3. (Color online) Circular dichroism spectra of n CB ($n = 3, 5, 7$) molecules. Extinction unit, $10^4 \text{ dm}^3 \text{ mol}^{-1} \text{ cm}^{-1}$.

maxima at 213.48 nm. However, the corresponding rotatory strengths are 95.80 and 33.92, respectively. The strongest band has been observed from 200 to 225.78 nm with λ_{max} at 213.48 nm. Similarly, the 7CB molecule exhibits two absorption bands at 221.68 nm (λ_1) and 277.93 nm (λ_2). Furthermore, the strongest band has been observed from 205.86 to 237.50 nm with absorption maxima at 221.68 nm (λ_1).

D. Role of alkyl chains

The extinction coefficients corresponding to the absorption maxima, the HOMO and LUMO energies, and the energy gap (E_g) of isolated molecules have been reported in Table II. In order to understand the role of alkyl chains, the spectral characteristics of isolated single molecules have been

analyzed. Therefore, it may be concluded that the absorption maxima does not show any preference for an increment in the homolog number in both spectra. However, the substitution of two and four additional alkyl groups in 3CB (forming 5CB and 7CB, respectively) causes a drastic increment and decrement in the extinction coefficients as per the uv absorption spectrum, whereas, the extinction coefficients show a clear preference for homolog number as per the CD spectrum. A drastic increment has been noticed in the extinction coefficient with respect to the increment in homolog number. Thus, the substitution of two additional alkyl groups in 3CB (forming 5CB) causes a hypsochromic (blue) shift (in terms of λ) and a hyperchromic effect (in terms of absorbance). Furthermore, the substitution of four alkyl groups in 3CB (forming 7CB) leads to a bathochromic (red) shift and a hyperchromic effect. Similarly, an evaluation from 5CB to 7CB also shows a redshift and a hypochromic effect.

It may be noticed that the molecules show a clear preference for an increment in homolog number to exhibit HOMO and LUMO energies. However, the energy gap ($E_{\text{LUMO}} - E_{\text{HOMO}}$) also shows the same preference (Table II). An increment in the number of alkyl chains causes a decrement in the energy gap. Hence, the values of an energy gap for n CB ($n = 3, 5, 7$) molecules are independent of either redshift or blueshift. Molecular charge distribution analysis suggests that the phase stability also increases with respect to homolog number (Sec. III A). Furthermore, the maximum oscillator strength (f) and rotatory strength (R) in the uv region are directly proportional to the homolog number (Table III). The oscillator strength indicates the allowedness of electronic transitions in a molecule. Hence, the 7CB molecule is very flexible for electronic transitions. However, since the maximum oscillator strength of 5CB in the uv region has been obtained at longer wavelength regions, the uv stability of 5CB is higher than the other two molecules.

TABLE II. The extinction coefficients corresponding to absorption maxima (λ_{max}), HOMO, LUMO energies, and energy gap (E_g) of n CB ($n = 3, 5, 7$) molecules.

Molecule	λ_{max} (nm)		Extinction ^a		HOMO (eV)	LUMO (eV)	$E_g = (\text{LUMO}-\text{HOMO})$ (eV)
	uv-visible	CD	uv-visible	CD			
3CB	212.30	233.98	0.74	44.41	-8.35	-0.18	8.17
5CB	211.72	213.48	1.35	110.10	-8.46	-0.43	8.03
7CB	213.48	221.68	1.25	211.07	-8.33	-0.47	7.86
Dimer molecules							
3CB							
Stacking	211.72	212.30	1.27	313.12	-8.40	-0.35	8.05
In-plane	212.30	212.30	1.47	188.47	-8.42	-0.28	8.14
Terminal	212.30	212.89	1.56	390.63	-8.17	-0.04	8.13
5CB							
Stacking	210.55	212.89	2.29	434.35	-8.48	-0.58	7.90
In-plane	212.89	218.16	2.58	241.86	-8.53	-0.51	8.02
Terminal	211.72	212.89	3.16	1049.90	8.29	-0.23	8.06
7CB							
Stacking	215.23	214.65	2.68	508.54	-8.42	-0.57	7.85
In-plane	214.06	222.85	2.08	292.90	-8.39	-0.56	7.83
Terminal	214.06	219.34	2.68	29.18	-8.38	-0.52	7.86

^aExtinction unit, $10^4 \text{ dm}^3 \text{ mol}^{-1} \text{ cm}^{-1}$.

TABLE III. The maximum transition oscillator strength (f), rotary strength (R), and corresponding wavelengths for isolated molecules and dimer complexes of n CB ($n = 3,5,7$) molecules at the TD-DFT-B3LYP-6-31 + G (d) level of approximation.

Molecule	λ (nm)	f	λ (nm)	R
3CB	210.5	0.39	234.1	44.43
5CB	280.2	0.63	213.1	95.80
7CB	211.4	0.68	221.8	211.11
Dimer molecules				
3CB				
Stacking	210.1	0.57	211.5	215.95
In-plane	209.7	0.65	210.8	123.65
Terminal	227.6	0.73	212.4	192.24
5CB				
Stacking	280.4	1.01	211.8	351.21
In-plane	280.5	1.22	218.5	232.54
Terminal	281.2	1.45	212.3	951.61
7CB				
Stacking	216.8	1.04	214.3	278.30
In-plane	211.1	0.95	222.7	292.47
Terminal	211.7	1.37	221.7	18.20

E. Intermolecular interactions between a pair of molecules

The results obtained for isolated molecules suggest that the optical properties are influenced by their electronic structures. Therefore, in order to understand the self organizing ability of mesogens, the different types of molecular interactions have

been taken into consideration between a pair of n CB ($n = 3,5,7$) molecules. The interaction energies of dimer complexes have been considered to investigate the most energetically stable configuration in each mode. Furthermore, the optical properties of dimer complexes have also been reported in Table II. LCs are not isotropic, and clearly intermolecular interactions strongly influence their phase behavior, stability, and properties. Therefore, the interpretation of physical measurements on LCs in terms of molecular properties is a difficult problem. Hence, the basic idea underlying the study of molecular conformations is to show the physical and chemical properties of compounds that are closely related to the preferred conformations.

The conformational behavior of LCs displays a large variation in intermolecular effects and depends on the nature and magnitude of interactions. Each conformation may have distinct energy, and lower energy conformations will be populated in preference to those of higher energy. The most energetically stable configurations of n CB ($n = 3,5,7$) molecules during the different modes of interactions have been reported in Figs. 4–6, respectively. The comparison of stacked dimers between the molecules suggests that the extension of the chain length causes a recognizable segregation of the dimers into a perfect layer structure with strong parallel orientation. However, mutual interaction between the dimers in this structure is quite strong, in particular, to chain atoms. Moreover, the comparison of planar dimers indicates highly tilted structures with respect to extension of chain length, which favors translational motion in a molecular pair along the planar axis. Furthermore, the mutual interactions in these structures are quite weak. Hence, the end chains provide enough disorder in the crystal structure to pass on to nematic phase. Since, the tiltedness of the planar dimers increases with the extension of chain length,

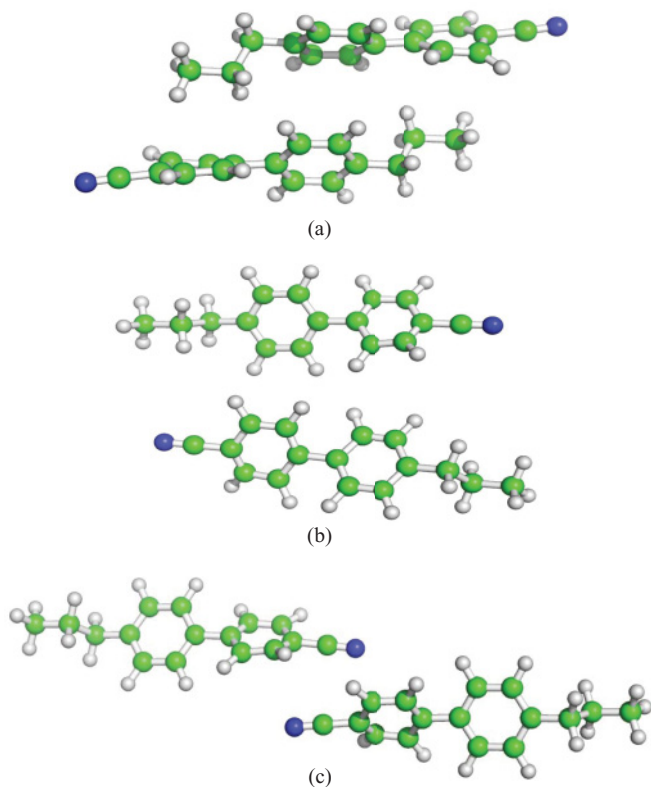


FIG. 4. (Color online) Energetically favorable structures of a 3CB dimer in (a) stacking, (b) in-plane, and (c) terminal interactions.

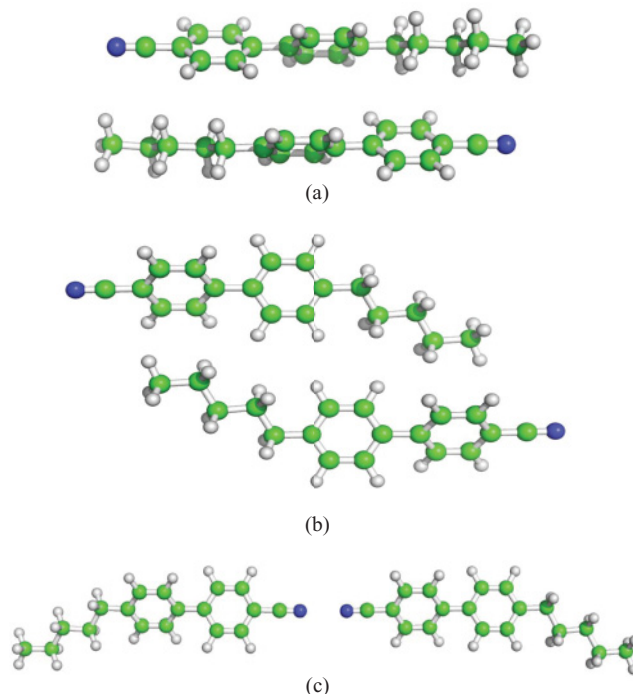


FIG. 5. (Color online) Energetically favorable structures of a 5CB dimer in (a) stacking, (b) in-plane, and (c) terminal interactions.

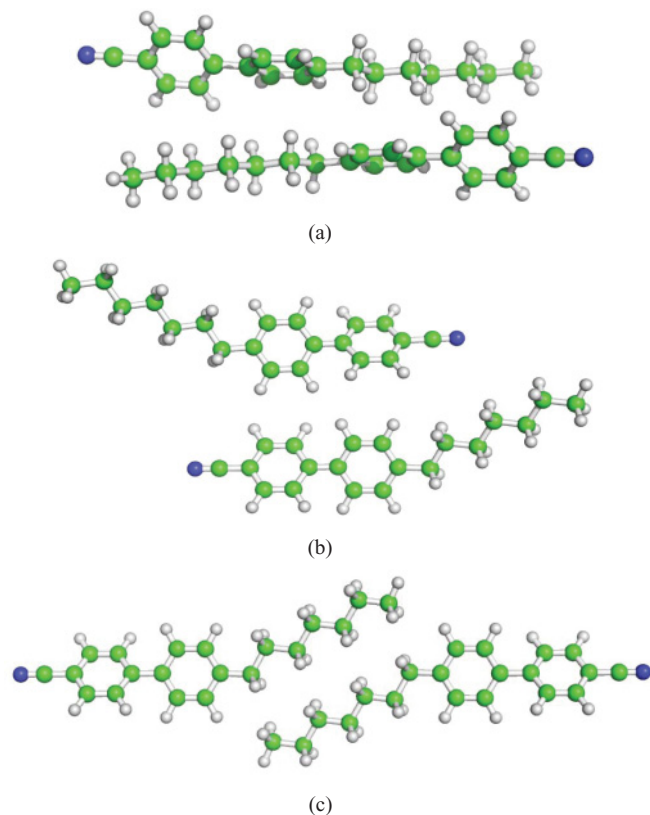


FIG. 6. (Color online) Energetically favorable structures of a 7CB dimer in (a) stacking, (b) in-plane, and (c) terminal interactions.

molecules will attain sufficient flexibility to move along their planar axis. Hence, the phase stability is expected to be high with the extension of the chain length. This supports the molecular charge distribution analysis reported in this paper. On the basis of interaction energy during the different modes of molecular interactions, the stability of dimer complexes of n CB molecules can be expressed as stacking, $3CB >$

$7CB > 5CB$; in-plane, $7CB > 3CB > 5CB$; and terminal, $7CB > 3CB > 5CB$.

IV. CONCLUSIONS

The salient features of the present work are:

(1) The electronic absorption and CD spectra of alkyl CN-biphenyls have been studied. All the molecules show strong absorption bands in the uv region. The maximum absorption wavelength (λ_{max}) has been obtained for 7CB in the uv-visible spectrum, while for 3CB, it has been obtained in the CD spectrum.

(2) The molecules show an apparent preference for $\pi \rightarrow \pi^*$ transitions. Furthermore, $\pi \rightarrow \pi^*$ transitions contribute higher oscillator and rotatory strengths.

(3) Alkyl chains play a dominant role in molecular properties and spectral characteristics. The absorption maxima and extinction coefficients do not show any preference for alkyl chain length, whereas, the energy gap values of isolated single molecules show a prominent preference for an increment in alkyl chain length. Similarly, the maximum oscillator and rotatory strengths in the uv region increase as the alkyl chain length increases.

(4) Although, the allowedness of electronic transitions is maximum for 7CB (68%) (Table II), the 5CB molecule exhibits high uv stability. The maximum oscillator strength occurs at a longer wavelength region compared to the other two molecules.

(5) Since the tiltedness of the planar dimers increases with the extension of chain length, molecules will attain sufficient flexibility to move along their planar axis. Hence, the phase stability is expected to be high with the extension of chain length. This supports the results obtained from molecular charge distribution analysis.

ACKNOWLEDGMENTS

The financial support rendered by the DST, CSIR, and UGC, New Delhi, India is gratefully acknowledged.

-
- [1] P. L. Praveen and D. P. Ojha, *Mater. Chem. Phys.* **126**, 248 (2011).
- [2] Z. Zhang and H. Guo, *J. Chem. Phys.* **133**, 144911 (2010).
- [3] M. Castari, A. Bosco, and A. Ferrarini, *J. Chem. Phys.* **131**, 054104 (2009).
- [4] K. Hori and N. Kouno, *Acta Crystallogr. Sect. C: Cryst. Struct. Commun.* **65**, o108 (2009).
- [5] B. Martínez-Haya and A. Cateos, *Phys. Rev. E* **81**, 020701(R) (2010).
- [6] T. Geelhaar, K. Tarumi, and H. Hirschmann, *SID Tech. Dig.* **27**, 167 (1996).
- [7] Y. Goto, T. Ogawa, S. Sawada, and S. Sugimori, *Mol. Cryst. Liq. Cryst.* **209**, 1 (1991).
- [8] G. W. Gray, K. J. Harrison, and J. A. Nash, *Electron Lett.* **9**, 130 (1973).
- [9] R. Dabrowski, *Mol. Cryst. Liq. Cryst.* **191**, 17 (1990).
- [10] W. Koch and M. C. Holthausen, *A Chemist's Guide to Density Functional Theory* (Wiley-VCH, Weinheim, 2000).
- [11] H. L. Peng, J. L. Payton, J. D. Protasiewicz, and M. C. Simpson, *J. Phys. Chem. A* **113**, 7054 (2009).
- [12] W. Haase, H. Paulus, and R. Pendzialek, *Mol. Cryst. Liq. Cryst.* **100**, 211 (1983).
- [13] I. Zgura, R. Moldovan, T. Beica, and S. Frunza, *Cryst. Res. Technol.* **44**, 883 (2009).
- [14] P. Hohenberg and W. Kohn, *Phys. Rev.* **136**, B864 (1965).
- [15] W. Kohn and L. J. Sham, *Phys. Rev.* **140**, A1133 (1965).
- [16] R. O. Jones and O. Gunnarsson, *Rev. Mod. Phys.* **61**, 689 (1989).
- [17] M. C. Zerner, *Rev. Comput. Chem.* **2**, 313 (1991).
- [18] M. C. Zerner, in *Semiempirical Molecular Orbital Methods*, edited by K. W. Lipkowitz, R. Larter, and T. R. Cunsari (Wiley-VCH, New Jersey, 2004), p. 153.
- [19] M. Kuribayashi and K. Hori, *Liq. Cryst.* **26**, 809 (1999).

- [20] P. L. Praveen and D. P. Ojha, *Mol. Cryst. Liq. Cryst.* **528**, 178 (2010).
- [21] P. L. Praveen and D. P. Ojha, *J. Mol. Liq.* **158**, 27 (2011).
- [22] P. T. Lin and S. T. Wu, *Mol. Cryst. Liq. Cryst.* **411**, 243 (2004).
- [23] H. F. Hsu, S. J. Chien, H. H. Chen, C. H. Chen, L. Y. Haung, C. H. Kuo, K. J. Chen, C. W. Ong, and K. T. Wong, *Liq. Cryst.* **32**, 683 (2005).
- [24] T. Hanemann, M. C. Bohm, W. Haase, and S. T. Wu, *Liq. Cryst.* **11**, 917 (1992).
- [25] Z. Markovic, N. Manojlovic, and S. Zlatanovic, *J. Ser. Soc. Comp. Mech.* **2**, 73 (2008).
- [26] U. Quotschalla, T. Hanemann, M. C. Bohm, and W. Haase, *Mol. Cryst. Liq. Cryst.* **207**, 103 (1991).
- [27] I. C. Khoo and S. T. Wu, *Optics and Non Linear Optics of Liquid Crystals* (World Scientific, Singapore, 1993).
- [28] P. Yeh and C. Gu, *Optics of Liquid Crystal Displays* (Wiley, New Jersey, 2010).
- [29] M. Mizuno and T. Shinoda, *Mol. Cryst. Liq. Cryst.* **56**, 111 (1979).